Characterization of the scientific grade Hawaii detector for LIRIS

José Acosta–Pulido[a], Carlos Dominguez–Tagle[a] and Arturo Manchado[a]

[a]Instituto de Astrofisica de Canarias, 38200 La Laguna, SPAIN

ABSTRACT

The instrument LIRIS is a near IR spectrograph to be installed at the WHT telescope. Currently it is being assembled at the Instituto de Astrofisica de Canarias. The instrument will have a Hawaii 1K×1K array as the detector. Here we report the laboratory characterization of the scientific grade unit. We give the relevant parameters such as linearity range, gain and readout noise. These results confirm that the science grade detector will fulfil the astronomical requirements for making LIRIS a front line IR instrument. We also discuss some peculiar effects which need to be taken into account in order to guarantee a correct astronomical performance. Among these effects we consider: variation of the dark signal with integration time, cross–talk, and persistance. We also discuss the variation of the bias level with detector temperature and the need to establish an extremely stable control of the temperature.

Keywords: Detector characterization, IR instrumentation, IR astronomy

1. INTRODUCTION

LIRIS is a near IR spectrograph under construction at the Instituto de Astrofisica de Canarias. It will be operating at the 4.2 m WHT located at the Observatorio del Roque de Los Muchachos (Canary Islands). For more details see the paper presented by Manchado et al (these proceedings). Here we will describe the results of the tests performed to the science grade 1024x1024 IR Hawaii detector by Rockwell.

The controller system for the Hawaii detector uses the SDSU (San Diego State University) controller supplied by IRLabs (Tucson, AZ). A modified DSP code developed by P. Moore of the Isaac Newton Group for the Ingrid Project* is being used. This code includes reading modes such as Fowler sampling and Follow–UP–the–Ramp . The SDSU controller communicates with the control computer through two optical fibers, receiving elementary commands at 4 MHz and transmitting status and/or data at 50MHz. In the present version the four quadrants of the detector are driven at the same time with a reading rate of 3 msecs/pixel, leading to a time of 0.9 seconds for a complete frame readout.

2. TEST CRYOSTAT

A test cryostat was designed at the IAC to check and characterize our detector system (see Fig. 1). The cryostat has a liquid nitrogen tank, which mantains a stable temperature of $\simeq$ 77 K at the cold plate. The detector and its fanout board are connected to the cold plate through a thermal link, reaching a minimum temperature about 80 K. This thermal link has also the function to slow down the cooling and heating rates (below 4K/hour) of the detector during the cryostat cooling and warming processes, in order to avoid its mechanical breaking. Inside the cryostat there is a small filter wheel with four possible selections (usually the filters J, H and K_s plus a cold dark slide). Behind the entrance window there is removable cold mask with a central pin–hole. These basic mechanisms allow to test the detector under different illumination conditions: roughly dark, uniform illumination using the pinhole and completely open to form images by placing external lenses.

Further author information: (Send correspondence to J.A.P.)
J.A.P.: E-mail: jap@ll.iac.es, Telephone: +34 922605266
C.D.T.: E-mail: carlosd@ll.iac.es, Telephone: +34 922605200
A.M.T.: E-mail: amt@ll.iac.es, Telephone: +34 922605239
*http://www.ing.iac.es/Astronomy/instruments/ingrid/index.html

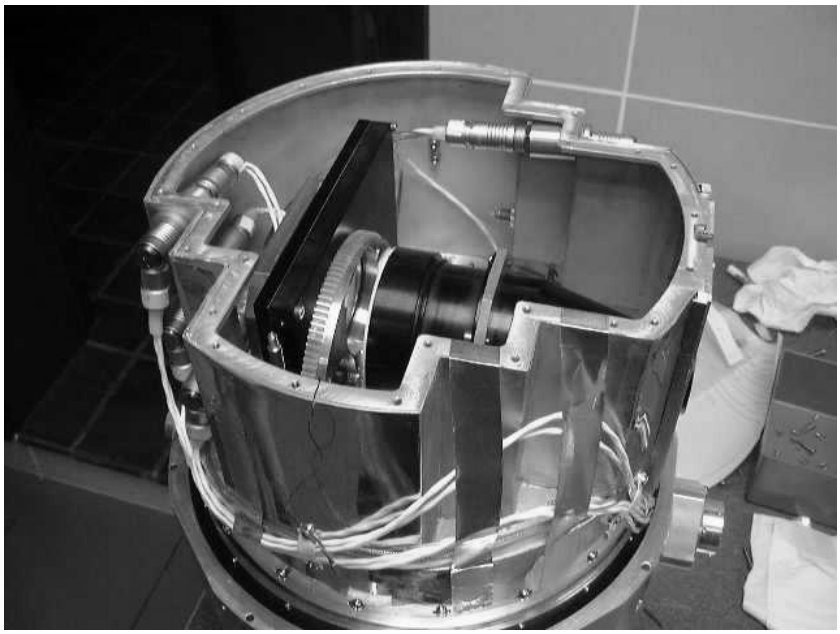

Figure 1. The test cryostat without the top cover. The fan–out box with the detector inside can be distinguished on the left side. The filter wheel is placed just behind the box.

In the final configuration of the LIRIS instrument the detector will be cooled down to a temperature of $\sim$ 65 K using the second stage of a Closed Cycle Cooler. In this case the temperature stability is not as good as in the case of LN_2, and for this reason a temperature controller (Lakeshore –340) will be used to stabilize the detector temperature within few mK. Such strong requirement is imposed due to the strong variation of the bias with the detector temperature (discussed in Section 8).

3. LINEARITY RANGE

The linearity range was established using a sequence of flat–field exposures where the integration time was increased until the saturation level was reached. A black–body was used as the illumination source. The stability of the black–body was checked by repeating reference frames during the sequence. A dark frame of the same exposure time was subtracted to each flat–field image, this step was turned on to be critical for short exposure times (see section 6). Each dark subtracted frame was divided by the exposure time and finally normalize to a median value of the illumination flux. The resulting linearity curves are presented in figure 2. The linear regime, where the deviation is below 1%, covers until 10000 ADUs, which implies a range of 60000 e^-, using the values for the gain derived below. The full well depth extends until 35000 ADU, which implies a value of 210000 e^-

4. GAIN CALIBRATION

The detector system gain has been calibrated by measuring the shot noise varying the detector signal at high photon flux levels. In order to minimize the pixel–to–pixel variations we have used differences of uniformly illuminated images taken successively and at the same light level. In this way the gain (e^-/ADU) can be estimated from the following expression:

$$g = \frac{mean(flat1 + flat2)}{Variance(flat1 - flat2)},$$

in which the readout noise is considered negligible against the photon shot noise. We plotted in Figure 3 the variance of the frame difference versus the mean of the frame coaddition signal for each quadrant for a set of

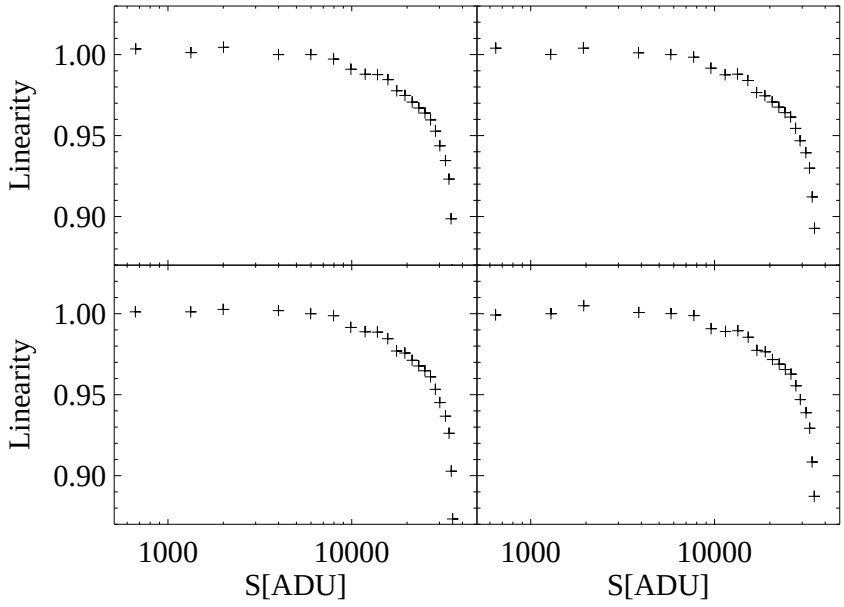

Figure 2. Linearity deviations, the abscissae axis represent the ratio between the observed to the linear value. Each panel represents a quadrant of the detector.

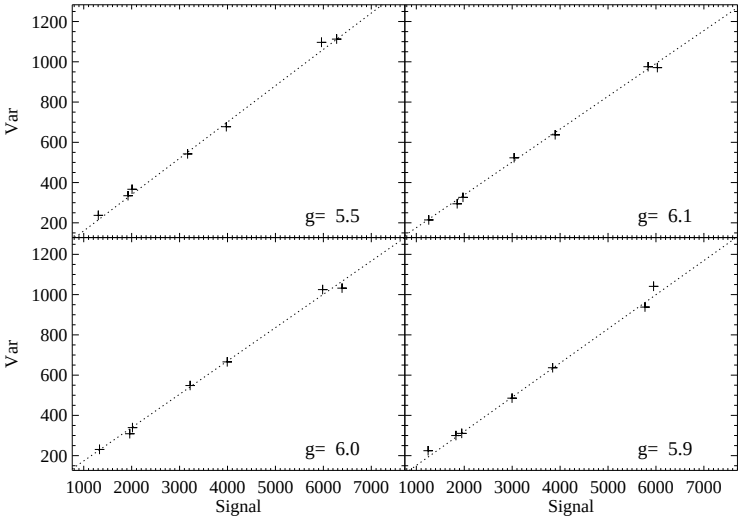

Figure 3. Gain determination based on the difference between two consecutive flat–field images.

measurements within the linear regime. The inverse slope of the linear fit gives the value of the pixel transfer function in e^{-1}/ADU. A value around $6e^{-}$/ADU has been obtained for all quadrants.

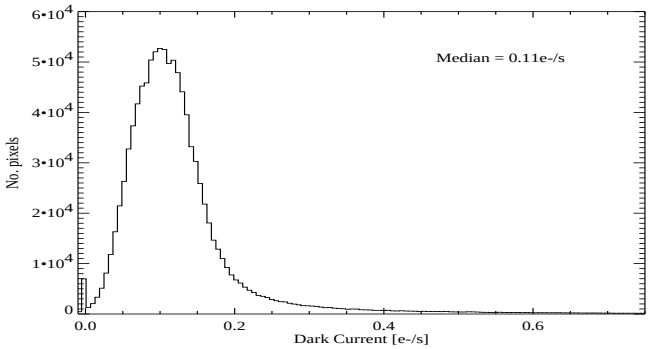

Figure 4. Dark current histogram. The tail at the right of the peak corresponds to the warm to hot pixels.

5. DARK CURRENT

The dark current of the detector is a key parameter for low background applications such as spectroscopy of very faint objects. The dark current was measured in the best conditions we could achieved with our setup. The cold dark slide plate was put in front of the detector and the pinhole behind the entrance window, in addition we placed a mirror in front of cryostat entrance window to block contamination by external radiation. A series of 1200 s dark exposures were obtained in Follow–Up–the–Ramp readout mode, reading the detector every two minutes. The distribution of dark current values for all pixels is shown in Fig. 4. The median value of the dark current is 0.019 ADU/s, which is equivalent to 0.11 e^{-1}/s. It is also found that 95 % of all pixels exhibits a dark current below 0.33 e^{-1}/s. The distribution presents an asimmetry towards the right, which corresponds to pixels with anomalously high dark current, also called hot pixels (see discussion below). It is expected that the dark current is lower by a factor 10 when the detector is operated at 65 K, according to temperature dependence described by Finger et al. (1997).[1]

5.1. Hot pixels

Most hot pixels are easily identified in the dark images since they appear as bright individual spots, their signal is well above the mean value of the frame. In addition, these pixels show a non–linear behaviour. For this reason, many of them cannot be detected in short measurements but they show up at long exposures. The number of hot pixels increases with the integration time, it goes from 0.15 to 0.8 % after 100 seconds (see Fig. 5. Nevertheless, there seems to be a limit to the number of hot pixels for measurements longer than 200 s (see report at INGRID Web page[†].

We have also learned that reading out the detector at high temperatures produces a sort of short–circuit at many pixels, which cannot be eliminate later when the unit is cool. During the first test series the detector was regularly read out while cooling down, starting when T$\sim$ 200 K until it reached the minimum temperature (T$\simeq$ 82 K). This was done in order to monitorize the adequate range of the bias voltage to be applied. At cold conditions, we noticed an excesively high number of hot pixels, about 25 % (see Fig. 6) of the total. In a given dark image, we mean by hot pixels those which are above 5σ of the median value. Later on, and following the suggestions from other team having experienced a similar problem we allowed to heat up the system and then we cooled down again but this time without powering up the detector. Surprisingly the high number of hot pixels was drastically reduced and the appearence was very clean (see Fig. 6) The current explanation for this behaviour is related to the manufacturing process at Rockwell, in particular when the detector surface is flatten (P. Moore, private communication).

[†]http://www.ing.iac.es/Astronomy/instruments/ingrid/index.html

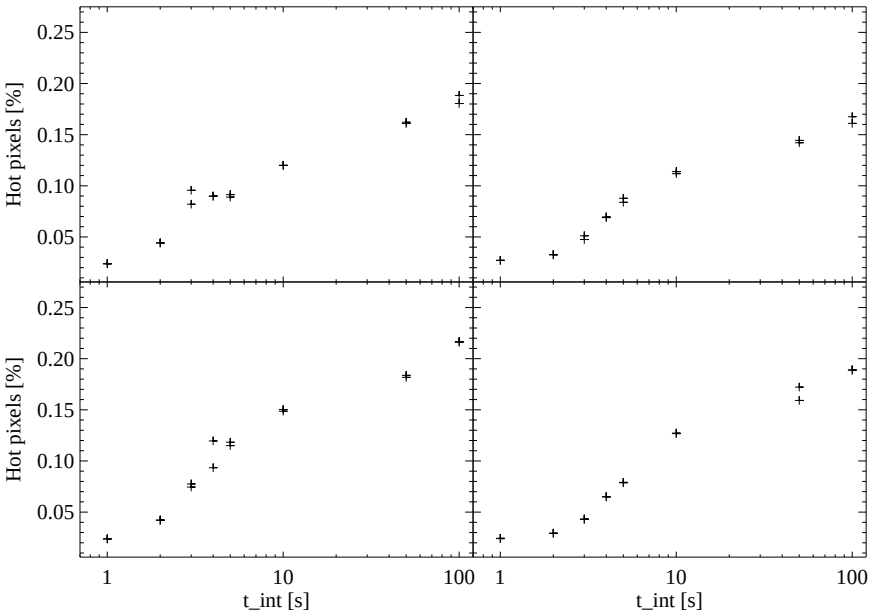

Figure 5. The number of hot pixels is represented as a function of the integration time. The hot pixels are obtained from dark exposures, as those pixels in which the signal is 5σ above the median value.

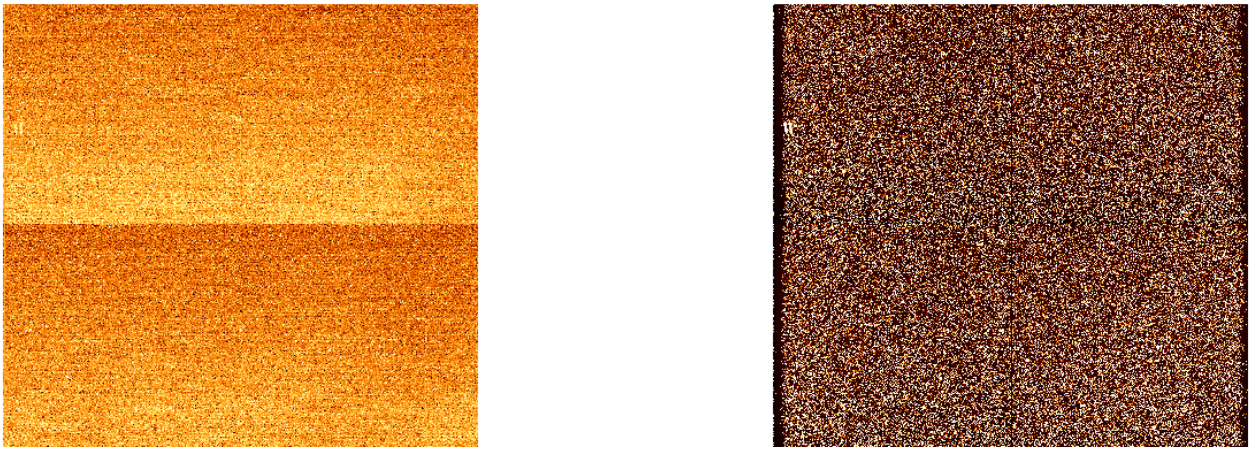

Figure 6. Both images correspond to a dark exposure of 100 s integration time. The frame represented in the right panel corresponds to the first cooling down of the detector, when it was read in warm conditions. Note the very large number of hot pixels. The frame in the left panel corresponds to the second cooling down, when it was read only at cold conditions. The number of hot pixels has been reduced dramatically.

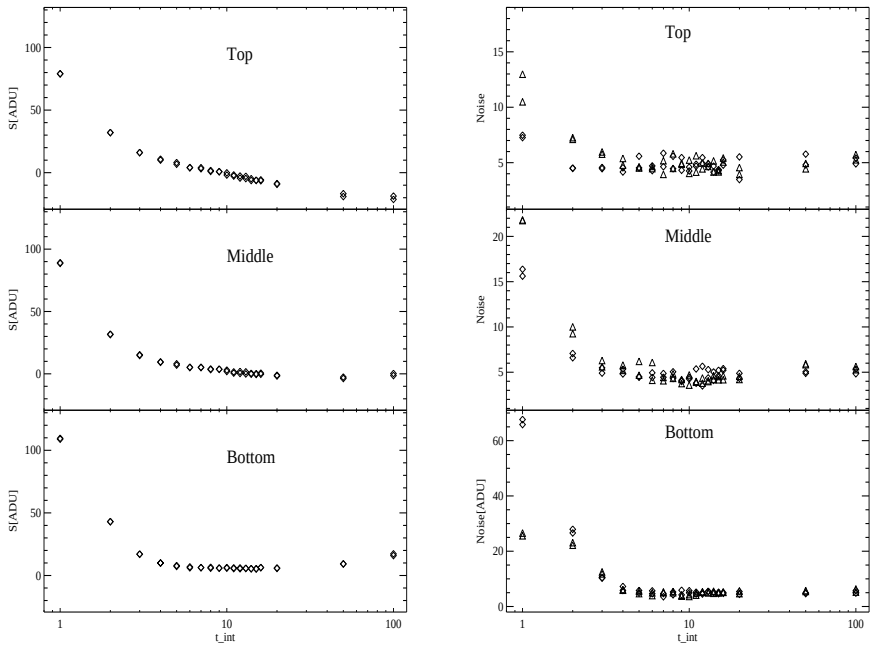

Figure 7. Signal offset (left panel) and noise (right panel) variation with integration time across the detector quadrant. The noise is measured as the sigma values scaled from the first and third quartiles.

6. THE RESET ANOMALY

We have noticed that dark exposures of very short integration times show an offset signal which cannot be eliminated and decreases from 100 ADU at $t_{int} = 1$ s to a value close to zero after 10 s. Moreover this behaviour differs depending on the row (the slow clock signal) across the quadrant (see Fig 7). At the top of the quadrant, which coincides with the first pixels to be addressed, the offset continuosly decreases up to 100 s. Instead at the bottom the offset shows a minimum at $\sim$ 10 s and then starts to increases very slowly. The net effect on the image of a dark exposure at large integration time is a vertical shadowing (see Fig. 8). At short integration time ($t_{int} < 3$ s) the image shows a fan–like pattern which has been found to be relatively constant over time (see Fig. 8). The noise as measured by the pixel–to–pixel variations is large at the integration time of 1 s, whereas it decreases to a minimum value at $\sim$ 10 s (see Fig. 8). This effect has been previously reported in the same type of IR detectors by Finger et al. (2000).[2] They attributed the effect to strong non–linearities introduced after the integrating capacity is reset.

7. READOUT NOISE

We have described above that dark exposures taken with short integration times present a noise pattern which decreases with a timescale of about 10 s. For that reason the readout noise has been estimated from dark measurements obtained with 10 s exposure time, using double correlated readouts. The resulting value is $\sim$ 4.5 ADU, including both readouts. This corresponds to a value of 27 e^- for the two readouts and 20 e^- for a single readout, using for the gain the values quoted above.

7.1. Sampling strategies and noise reduction

The readout noise can be reduced by increasing the number of readouts either in multiple non–destructive readouts (Fowler sampling) or in the Follow–Up–The–Ramp sampling schemes. Due to software limitations our

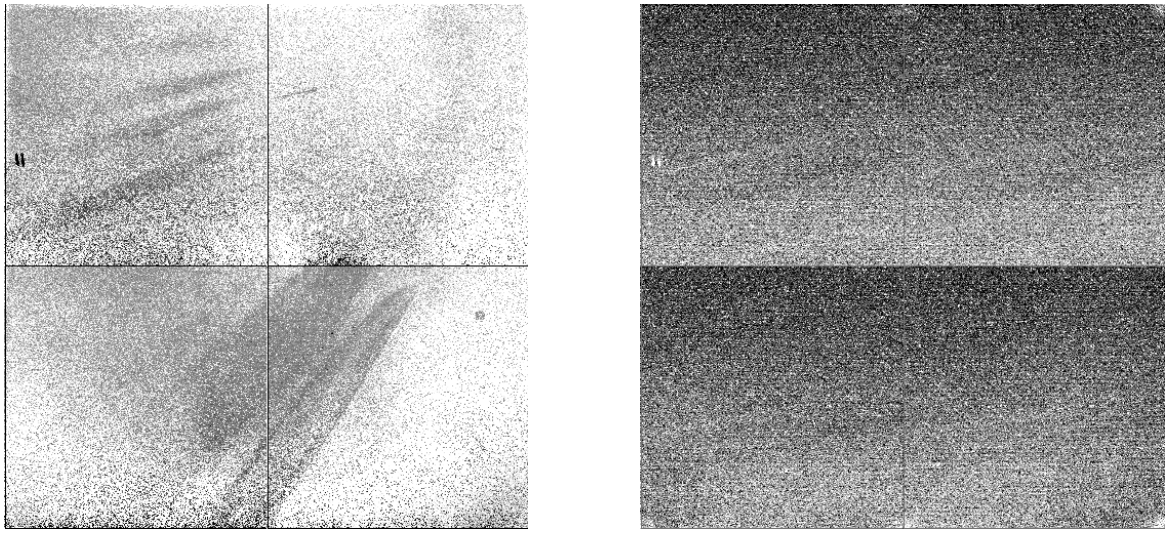

Figure 8. Right panel: Dark signal taken with 10s integration time. A shadowing effect is clearly seen with the gradient along the slow clock signal. Left panel: Dark signal taken with 1 s integration time. A fan–like structure is present in the images, which introduces an undesired noise pattern.

system has a maximum number of 16 readouts, which effectively reduces the readout noise by a factor 4.

7.2. Multiplexer Glow

The use of readout schemes which perfom multiple non–destructive readout during an exposure increase the perfomance when measuring low flux levels (as shown above). However it can be seen that a shot noise appears when the number of readouts is largely increased. Finger et al (2000)[2] concluded that this effect is due to the shift registers glow. Despite the low number of readout allowed in our system we have investigated the influence of such noise. We have found that the large effect of the glow is found at the junction of the quadrants and slightly less at the corners, it reaches a value of $\sim 40 ADUs$ after 16 readouts. However this effect remains below 2 ADU in the central region of the detector.

8. TEMPERATURE DEPENDENCE OF BIAS VOLTAGE

We have investigated the dependence of the bias voltage, the pre–integration value with the temperature. For that purpose we have set our detector temperature controller to a temperature few degrees higher than the LN_2 stable situation. We have monitorized the variation of the bias voltage as a function of the temperature, the results of one experiment is shown in Figure 9. It can be seen that the bias voltage follows the same trend as the measured temperature, but showing a long estabilization time. Unfortunately due to high inertia of the thermal link the temperature sensor does not represent the current detector temperature. By looking at the absolute variation of temperature and bias voltage we infer a variation of $\sim$ 170 ADU/K, which imposes a stability of the detector temperature below 5 mK in order to have a bias variation of 1 ADU.

.1. A note on the data analysis

In order to characterize the distribution of data points we have frequently used the median as the representative value. The width of the distribution is computed from the difference of the quartiles to the median value. The lower quartile is the median of the lower half of the data, whereas the upper quartile is the median of the upper half of the data. For a normal distribution the following expressions are valid: $upper_quart - median = lower_quart - median$ and $\sigma_{norm} = 1.47 \times (upper_quart - median)$. We have used these statistical estimators because they are more robust against deviant data values.

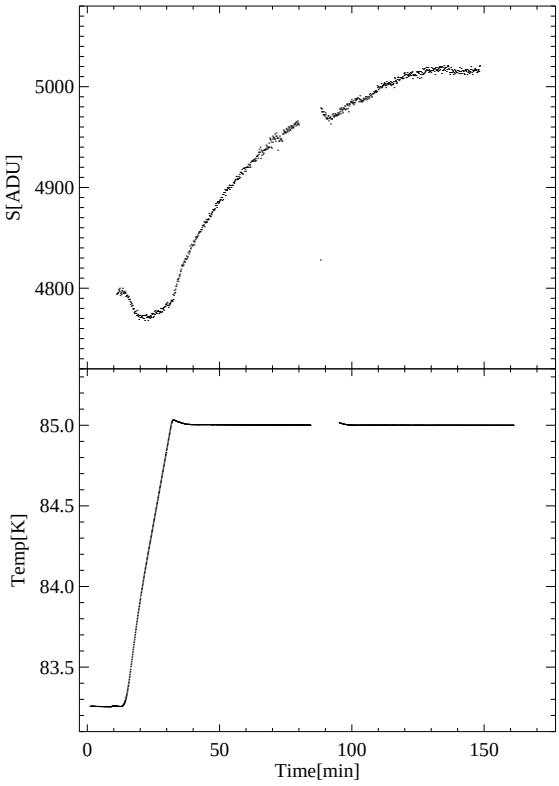

Figure 9. Variation of the bias as function of the temperature.

ACKNOWLEDGMENTS

We thank all members of the LIRIS project and especially Ezequiel Ballesteros. We also acknowledge P. Moore for his support.

REFERENCES

1. G. Finger, P. Biereichel, J. Lizon, M. Meyer, A. Morwood, G. Nicolini, and A. Silber, "Megapixel infrared arrays at the european southern observatory," in *Optical Telescopes oftoday and Tomorrow*, A. Ardeberg, ed., *Proc. SPIE* **2871**, pp. 1160–1170, 1997.
2. G. Finger, H. Mehrgan, M. Meyer, A. Morwood, G. Nicolini, and J. Stegmeier, "Performance of large format hgcdte and insb arrays for low background applications," in *Optical and IR Telescope Instrumentation and Detectors*, M. Iye, ed., *Proc. SPIE* **4008**, pp. 1280–1297, 2000.